

Performance Limitations in the R^3T Optical Random Access CDMA Protocol

Ziad A. El Sahn
Student Member, IEEE

Yousef M. Abd-El Malek
Student Member, IEEE

Hossam M. H. Shalaby
Senior Member, IEEE

El-Sayed A. El-Badawy
Senior Member, IEEE

Abstract – The effect of both noise and dispersion on the performance of the optical code-division multiple-access (OCDMA) round robin receiver/transmitter (R^3T) protocol is examined. Several performance measures, namely, the steady state system throughput, the protocol efficiency, and the average packet delay are evaluated. Our results reveal that there is performance degradation in the R^3T protocol. We found out that there are optimum values for the operating wavelength and the average peak laser power of the transmitter to compensate for this degradation.

I- INTRODUCTION

Nowadays as more and more users start to use data network, and their usage patterns evolve to include more and more bandwidth-intensive networking applications such as data browsing on the world wide web, java applications, video conferencing, ...etc., there emerges an acute need for high bandwidth transport network facilities, which are much beyond those that current high-speed networks can provide. The optical code-division multiple-access (OCDMA) which constitutes the backbone of the next generation of the internet [1] – [11] is the one that gives the highest system resources utilization. This is due to the extra-high bandwidth offered by optical links and optical signal processing speed bestowed by the optical components.

Most efforts in the area of optical direct detection CDMA have been concentrated on the physical layer [1], [2]. The performance analysis of the slotted and unslotted fiber optic CDMA has been studied in [3], [4]. Two protocols with and without pretransmission coordination have been proposed for slotted optical CDMA packet networks in [5]. However the effect of multi-packet messages, connection establishment and corrupted packets haven't been taken into account. Recently, Shalaby [6] has developed a new protocol called round robin receiver/transmitter (R^3T) protocol that has solved some of the above problems. The R^3T protocol is based on a go-back n automatic repeat request (ARQ), that is when a packet gets corrupted, the transmitter retransmits it and all sub-sequent packets. This scenario gives good performance for low population networks, while the performance is still low for larger population networks. Considering only the retransmission of corrupted packets, a selective reject ARQ has been applied in [7], which yields to better results in case of higher population networks.

Our goal in this paper is twofold. First, we consider the effect of both shot noise and thermal noise on the performance of the R^3T protocol and compare our results with that in [6]. Our second aim is to investigate the effect of dispersion in optical fibers in limiting the user bit rate.

The rest of this paper is organized as follows; Section II is

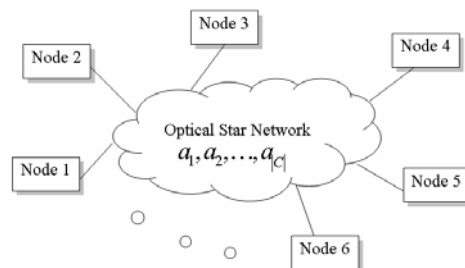


Fig. 1. Optical CDMA network architecture.

devoted for a basic description of the system architecture. A mathematical model and a basic description of the state diagram of the proposed R^3T protocol is outlined in Section III, where a derivation of the steady state system throughput under the effect of shot and thermal noise is given and compared with the ideal one. The effect of the light dispersion is then discussed. Section IV is maintained for the simulation results. Finally our conclusions are given in Section V.

II- SYSTEM ARCHITECTURE

A. Network Topology:

The basic architecture of our optical CDMA network is shown in Fig. 1, which represents a passive star network connecting N users.

B. Optical Orthogonal Codes:

A set of optical orthogonal codes (OOC's) $C=\{a_1, a_2, \dots, a_{|C|}\}$ with cardinality $|C|$ that depends on the code weight w , code length L , and both the autocorrelation and cross-correlation constraints λ_a, λ_c , respectively is used as the users signature sequences. Traditionally,

$$\lambda_a = \lambda_c = 1 \quad \Rightarrow \quad |C| = \left\lfloor \frac{L-1}{w(w-1)} \right\rfloor, \quad (1)$$

where $\lfloor x \rfloor$ denotes the largest integer not greater than x . Due to the bursty nature of the traffic, normally we have $N > |C|$ and users are assigned to OOC's according to one of the two protocols proposed in [5]. Furthermore, the code is randomly cyclic shifted around itself once assigned for interference control purposes.

C. Optical CDMA Protocol:

In the R^3T protocol many assumptions were imposed [6]. Briefly, time is slotted with slot size T_s , a message is composed of ℓ packets each having K bits. Each node has a single buffer to store only one message, connection requests

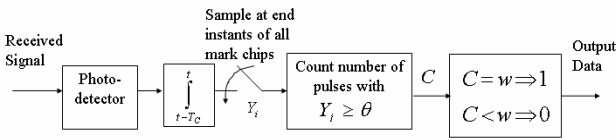


Fig. 2. Chip-level receiver model.

and acknowledgements are exchanged between stations, finally the ARQ used is a go-back n protocol and the two-way propagation time is assumed to be equal to t time slots.

D. Chip-level Receiver:

Chip-level receivers are used because of their high ability to overcome the effect of multiple-access interference (MAI). The complete model for this receiver can be found in [8], a simplified block diagram of this receiver is shown in Fig. 2.

Assuming that there are $r \in \{1, 2, \dots, N\}$ active users, we

define $k \in \{0, 1, 2, \dots, r-1\}$, such that $k = \sum_{i=1}^w k_i$, and

$m \in \{0, 1, \dots, r-1-k\}$ as the number of users that interfere with the desired user at exactly 1 chip and w chips, respectively; k_i denotes the number of users that interfere with the desired user at weighted chip i .

The conditional packet success probability for the chip-level receiver is expressed as follows;

$$P_S(r/m, \bar{k}) = [P_{bc}(m, \bar{k})]^k, \quad (2)$$

where $\bar{k} = \{k_1, k_2, \dots, k_w\}$ is the interference vector and $P_{bc}(m, \bar{k})$ is the bit correct probability. The packet success probability is thus given by:

$$P_S(r) = \sum_{k=0}^{r-1} \sum_{m=0}^{r-1-k} \frac{(r-1)!}{k!m!(r-1-m-k)!} \cdot p_1^k p_w^m (1-p_1-p_w)^{r-1-m-k} \cdot \sum_{\substack{k_1, k_2, \dots, k_w \\ k_1 + \dots + k_w = k}} \frac{k!}{k_1! \dots k_w!} \cdot \left(\frac{1}{w}\right)^k \cdot [P_{bc}(m, \bar{k})]^k. \quad (3)$$

Here, p_1 and p_w denote the probability of 1 and w chip-interferences, respectively between two users [6]:

$$p_w = \frac{1}{L} \cdot \frac{1}{|C|} = \frac{1}{L} \cdot \left[\frac{L-1}{w(w-1)} \right]^{-1}. \quad (4)$$

$$p_1 = \frac{w^2}{L} - w p_w$$

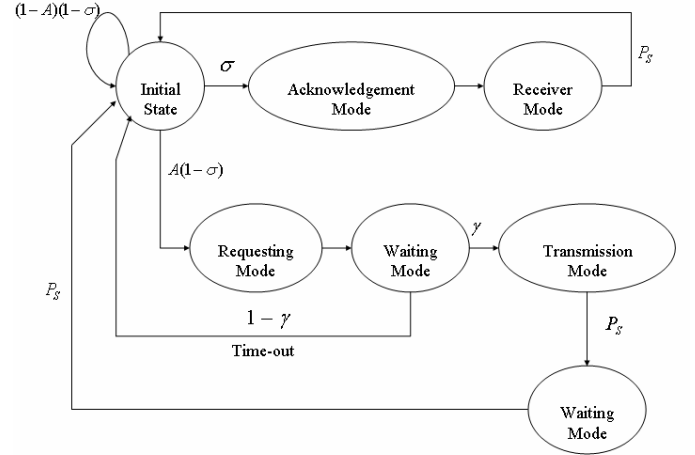
The bit correct probability of the chip-level receiver considering only the effect of the MAI has been derived in [5]:

$$P_{bc}(m, \bar{k}) = \frac{1}{2} + \frac{1}{2^{m+1}} \left(\sum_{i=1}^w \frac{1}{2^{k_i}} - \sum_{i=1}^{w-1} \sum_{j=i+1}^w \frac{1}{2^{k_i+k_j}} + \dots + (-1)^{w-1} \frac{1}{2^k} \right). \quad (5)$$

III- MATHEMATICAL MODEL & THEORETICAL ANALYSIS

A. The R^3T 's State Diagram:

A simplified state diagram for the R^3T optical CDMA protocol is shown in Fig. 3. A user in the initial state scans across the codes in a round robin method, when a connection request is found, an event which happens with probability σ ,


 Fig. 3. State diagram of the R^3T optical CDMA protocol.

the user proceeds to send an acknowledgement and enters the receiver mode. When all packets are received successfully, event happening with probability P_S , the user returns to the initial state again. The station moves to the requesting mode from the initial state if no requests are found and if there is a message arrival, event that happens with probability A , also called the user activity. After asking for a connection request, the station enters a waiting mode till it receives an acknowledgement, event which occurs with probability γ , if timed-out (after τ time slots), the station returns to the initial state, otherwise it enters the transmission mode.

After the transmission is done, the station goes to the waiting mode to collect the acknowledgements of the last packets sent, and then it returns to the initial state again. The station remains in the initial state if there is no message arrival and if no connection requests are found.

Because of the complexity of the mathematical model given above, the equilibrium point analysis (EPA) was the technique used in [6] to measure the protocol performance namely, the steady state system throughput, the protocol efficiency and the average packet delay.

The steady-state system throughput $\beta(N, A, t, \tau, \ell)$ is defined as the average number of successful received packets per slot and is given by [6]:

$$\beta(N, A, t, \tau, \ell) = \frac{P_S(r_o) \ell \cdot r_o}{\ell + (1 - P_S(r_o)) \cdot (t \wedge \ell - 1) \cdot (\ell - t \wedge \ell / 2)}, \quad (6)$$

where $t \wedge \ell$ is defined as $\min\{t, \ell\}$ and r_o denotes the number of transmitting users in a given slot and is given by the solution of the following equation [6]:

$$N[\ell + (1 - P_S(r_o)) \cdot (t \wedge \ell - 1) \cdot (\ell - t \wedge \ell / 2)] = r_o \left[2t\ell(1 - P_S(r_o)) + (2t + 2\ell - 1)P_S(r_o) + \frac{P_S(r_o)}{\sigma} + A(t-1) \frac{1-\sigma}{\sigma} P_S(r_o) + \left\{ 1 - \left[1 - \frac{\sigma}{A(1-\sigma)} \right]^{\ell/\tau} \right\}^{-1} P_S(r_o) \right]. \quad (7)$$

The protocol efficiency η and the average packet delay D (measured in slots) are expressed as follows:

$$\eta = \frac{\beta(N, A, t, \tau, \ell)}{N/2} \quad (8)$$

$$D = \frac{NA}{\beta(N, A, t, \tau, \ell)}$$

Neglecting the effect of both noise and dispersion, and considering only the effect of MAI we can write the packet success probability by substituting (5) in (3) as follows:

$$P_S(r) = \sum_{k=0}^{r-1} \sum_{m=0}^{r-1-k} \frac{(r-1)!}{k!m!(r-1-m-k)!} \cdot P_1^k P_w^m (1-P_1-P_w)^{r-1-m-k} \cdot \sum_{\substack{k_1, k_2, \dots, k_w: \\ k_1 + \dots + k_w = k}} \frac{k!}{k_1! \dots k_w!} \left(\frac{1}{w}\right)^k \cdot \left[\frac{1}{2} + \frac{1}{2^{m+1}} \left(\sum_{i=1}^w \frac{1}{2^{k_i}} - \sum_{i=1}^{w-1} \sum_{j=i+1}^w \frac{1}{2^{k_i+k_j}} + \dots + (-1)^{w-1} \frac{1}{2^k} \right) \right]^K \quad (9)$$

Now we will study the performance of the R^3T protocol taking into account the effect of both shot and thermal noise, then the dispersion effect will be discussed. The only change in the throughput equation will be in the evaluation of the packet success probability or more precisely the bit correct probability.

B. Poisson Shot Noise Limited Photodetectors:

Assuming that the receiver's photodiode is the shot noise limited, the bit correct probability can be found in [5]. We have modified its form using the exclusion-inclusion principle to get this general form, which is more simple and suitable for simulations.

$$P_{bc}(m, \bar{k}) = \frac{1}{2} - \frac{1}{2} \sum_{b=0}^1 (-1)^b \cdot \sum_{i=1}^w (-1)^i \binom{w}{i} \cdot e^{-Qbi} \cdot \left(\frac{1}{2} + \frac{1}{2} e^{-Qi} \right)^m \cdot \left(\frac{1}{2} + \frac{1}{2} e^{-Q} \right)^{\sum_{j=1}^{k_j} k_j} \quad (10)$$

Here $b \in \{0,1\}$, is the data bit and Q denotes the average photon count per chip pulse which is related to the average photons per bit μ by,

$$Q = \frac{2\mu}{w} \quad (11)$$

C. Avalanche Photodetectors & Thermal Noise:

In our model we assume that the decision variable Y_j , for the chip-level receiver; which indicates the photon count per marked chip positions $j \in x = \{1, 2, \dots, w\}$ to have a Gaussian distribution and the decision threshold θ will have to be optimized [9]. Considering u users out of m users interfering in w chips and v_j users out of k_j users making interference at the weighted chip j , the conditional mean and variance m_{bj} and σ_{bj} , respectively are expressed as follows:

$$m_{bj} = G(u + b + v_j) Q + Q_d \quad (12)$$

$$\sigma_{bj}^2 = FGm_{bj} + \sigma_n^2$$

Here, G denotes the average APD gain, Q and Q_d are the average number of absorbed photons per received single-user

pulse and the photon count due to the APD dark current within a chip interval T_c , respectively and are given by [9]:

$$Q = \frac{RP_{av}T}{e \cdot w}, \quad Q_d = \frac{I_d T_c}{e} \quad (13)$$

Where, P_{av} is the received average peak laser power (of a single user), T is the bit duration, R is the APD responsivity at unity gain, I_d is the APD dark current, $h = 6.626 \times 10^{-34} J.s$ is Plank's constant and $e = 1.6 \times 10^{-19} C$ is the electron charge.

The variance of the thermal noise within a chip interval σ_n^2 is as follows,

$$\sigma_n^2 = \frac{2K_B T^\circ}{e^2 R_L} \cdot T_c \quad (14)$$

where, $K_B = 1.38 \times 10^{-23} J/K$ is Boltzman's constant, T° is receiver noise temperature, and R_L is the receiver load resistor.

Defining k_{eff} as the APD effective ionization ratio, the APD excess noise factor F can be written as;

$$F = k_{eff} G + \left(2 - \frac{1}{G} \right) (1 - k_{eff}) \quad (15)$$

We start by deriving the corresponding bit correct probability as follows:

$$P_{bc}(m, \bar{k}) = \frac{1}{2} \Pr\{\text{a bit success}/m, k, 1 \text{ was sent}\} + \frac{1}{2} \Pr\{\text{a bit success}/m, k, 0 \text{ was sent}\} \quad (16)$$

$$P_{bc}(m, \bar{k}) = \frac{1}{2} \Pr\{Y_j \geq \theta \text{ for all } j \in x/m, \bar{k}, 1 \text{ was sent}\} + \frac{1}{2} \Pr\{Y_j < \theta \text{ for some } j \in x/m, \bar{k}, 0 \text{ was sent}\}$$

Using the inclusion-exclusion property yielding to,

$$P_{bc}(m, \bar{k}) = \frac{1}{2} + \frac{1}{2} \sum_{b=0}^1 (-1)^b \times \Pr\{Y_j < \theta \text{ for some } j \in x/m, \bar{k}, b\} = \frac{1}{2} - \frac{1}{2} \sum_{b=0}^1 (-1)^b \sum_{i=1}^w (-1)^i \binom{w}{i} \Pr\{Y_1, Y_2, \dots, Y_j < \theta/m, \bar{k}, b\} \quad (17)$$

The last probabilities can be expressed as follows:

$$\Pr\{Y_1, Y_2, \dots, Y_j < \theta/m, \bar{k}, b\} = \sum_{u=0}^m \binom{m}{u} \left(\frac{1}{2}\right)^m \cdot \sum_{v_1=0}^{l_1} \binom{l_1}{v_1} \left(\frac{1}{2}\right)^{l_1} \cdot \sum_{v_2=0}^{l_2} \binom{l_2}{v_2} \left(\frac{1}{2}\right)^{l_2} \dots \cdot \sum_{v_i=0}^{l_i} \binom{l_i}{v_i} \left(\frac{1}{2}\right)^{l_i} \cdot \Pr\{Y_i < \theta/u, v_i, b\} \cdot \Pr\{Y_2 < \theta/u, v_2, b\} \dots \Pr\{Y_i < \theta/u, v_i, b\} = \sum_{u=0}^m \binom{m}{u} \left(\frac{1}{2}\right)^m \prod_{j=1}^i \sum_{v_j=0}^{l_j} \binom{l_j}{v_j} \left(\frac{1}{2}\right)^{l_j} Q\left(\frac{m_{bj} - \theta}{\sigma_{bj}}\right) \quad (18)$$

where $Q(x)$ is the normalized Gaussian tail probability

$$Q(x) = \frac{1}{\sqrt{2\pi}} \int_x^\infty e^{-s^2/2} ds \quad (19)$$

Combining last equations, we can get an expression for the bit correct probability as follows:

$$P_{bc}(m, k, b) = \frac{1}{2} - \frac{1}{2} \sum_{b=0}^1 (-1)^b \sum_{i=1}^w (-1)^i \sum_{u=0}^m \binom{m}{u} \left(\frac{1}{2}\right)^u \left(\frac{1}{2}\right)^{m-u} \cdot (20)$$

$$\prod_{j=1}^i \sum_{v_j=0}^{\ell_j} \binom{\ell_j}{v_j} \left(\frac{1}{2}\right)^{\ell_j} \mathcal{Q}\left(\frac{m_{bj} - \theta}{\sigma_{bj}}\right)$$

D. Dispersion Effect:

One of the main performance degradation factors in long-haul fiber optic communication systems is the dispersion effect, which results in temporal widening of optical pulses. In particular, intersymbol interference (ISI), pulse width and peak power limitation, and pulse distortion [10], [11] have previously been examined.

We focus our analysis upon the traditional pulse-distorting impact of the dispersion, which shows to be vital and severe in limiting the user bit rate. Modal dispersion and chromatic dispersion are the two mechanisms causing pulse spreading when selecting a graded index-multimode fiber.

Starting first with the modal dispersion, which is the main part that contributes in the light dispersion, the pulse spreading is:

$$\Delta t_{\text{modal}} = \frac{(NA)^4}{32 c \cdot n_1^3} \cdot z, \quad (21)$$

where NA denotes the numerical aperture of the fiber, n_1 is the refractive index of its core, $c = 3 \times 10^8$ m/s is the speed of light in free space and z is the fiber length or more precisely the interstation distance and is given by:

$$z = \frac{v \cdot t}{2} \times T_s \cdot \quad (22)$$

Here v is the velocity of light inside the fiber core and is related to its refractive index.

Then we consider the effect of the chromatic dispersion, which is the combination of both material dispersion and waveguide dispersion, we define the chromatic dispersion parameter as follows:

$$D(\lambda) = \frac{S_o}{4} \times \left[\lambda - \frac{\lambda_o^4}{\lambda^3} \right], \quad (23)$$

where λ is the operating wavelength, λ_o is the zero dispersion wavelength and S_o is the zero dispersion slope.

Let $\Delta\lambda$ be the spectral width of the used light source. The pulse spreading can be expressed by:

$$\Delta t_{\text{chrom}} = D(\lambda) \cdot \Delta\lambda \cdot z, \quad (24)$$

We finally, extended the slot duration to T_s' as depicted in equation (25) by including guard bands, to compensate for the ISI effect.

$$T_s' = KL \sqrt{T_c^2 + \Delta t_{\text{modal}}^2 + \Delta t_{\text{chrom}}^2}. \quad (25)$$

IV- NUMERICAL RESULTS

The packet success probability, the steady state system throughput, the average packet delay and the protocol efficiency derived above have been evaluated for chip level receivers taking into account the effect of MAI on the protocol's performance. The performance degradation

TABLE I
Typical Laser Link Parameters

Light Source	Optical Fiber	Photodetector	
<i>LED Source</i>	<i>Multimode Graded Index</i>	<i>APD</i>	
$\lambda = \{850, 1300, 1550\}$ nm	$NA = 0.257$ $n_1 = 1.478$	$R = 0.84$ A/W	$I_d = 1$ nA
$\Delta\lambda = 50$ nm	$S_o = 0.097$ ps/nm ² .km	$G = 100$	$R_L = 50$ Ω
	$\lambda_o = 1343$ nm	$K_{\text{eff}} = 0.02$	$T^\circ = 300$ °K

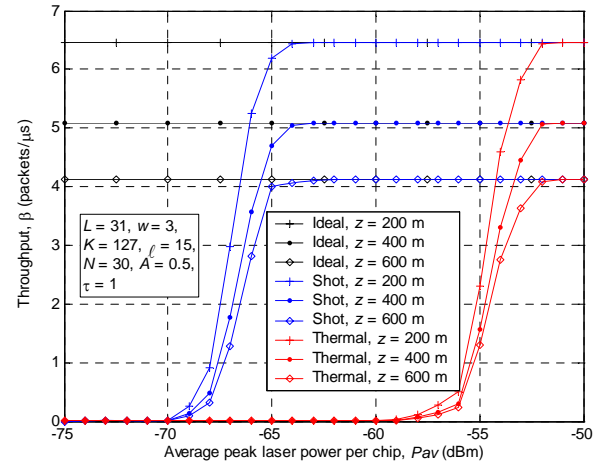


Fig. 4. Throughput vs. average peak laser power for different interstation distances.

parameters namely the shot noise, thermal noise at the receiver's photo-detector and the light dispersion in fibers are then considered.

Our results are plotted in Figs. 4-9. We have used OOC's with code length $L = 31$, and a code weight $w = 3$ in all figures. A packet size of $K = 127$ bits and a time out duration of $\tau = 1$ slot are also held constant. A time slot of $T_s = 1$ μ s is imposed in all figures but Fig. 9. Practical values of the interstation distances of $z \in \{200, 400, 600\}$ m have been selected. The remaining link parameters are stated in Table I.

In Fig. 4, the throughput has been plotted against the average peak laser power for different interstation distances, $z \in \{200, 400, 600\}$ m. General trends of the curves can be noticed. The throughput falls down as the interstation distance increases as in [6]. By increasing the average peak laser power up to -63 dBm (shot noise) or -51 dBm (thermal noise), regardless of the interstation distance, the receiver can tolerate the effect of the performance degradation and achieves the same throughput as the ideal case.

In Fig. 5, the throughput has been plotted versus the number of users for different arrivals of $A \in \{0.5, 0.02\}$. Similar trends of the curves can be noticed. There is always an optimum value of N that maximizes the throughput; also the position of this peak is shifted dramatically when changing the

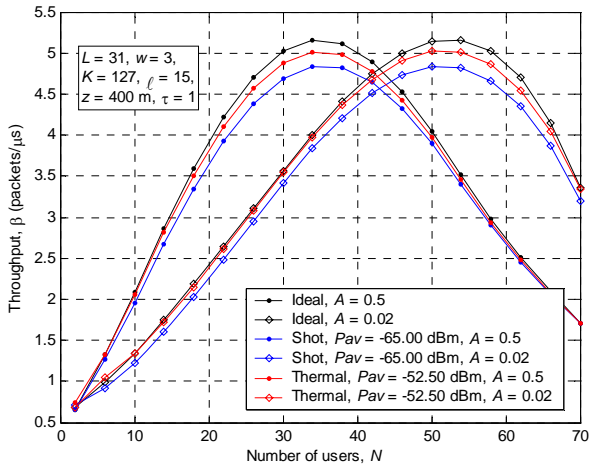


Fig. 5. Throughput vs. number of users for different activities.

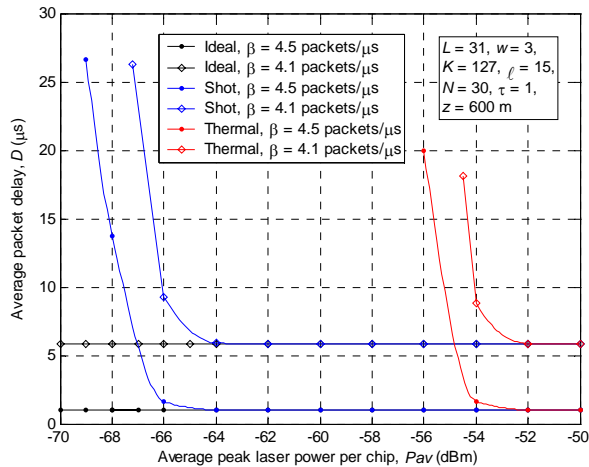


Fig. 6. Packet delay vs. average peak laser power for different throughput values.

average activity so as to maintain approximately a constant traffic in the network.

We have plotted the average packet delay versus the average peak laser power for different throughput values $\beta \in \{4.1, 4.5\}$ packets/ μ s, in Fig. 6. As in Fig. 4, the power levels must be increased to the same value, so that we can reach the optimum value of the delay at the required throughput.

Fig. 7, depicts the relation between the average packet delay and the throughput. It has been plotted for different values of average peak laser power. It can be seen, that in order to obtain negligible delay, the throughput will not be that high, so that a trade off must be considered. It can be inferred that because of the increase in the user activity, the throughput saturates [6] and the delay will grow rapidly.

We have plotted the protocol efficiency versus the message length ℓ for different average peak laser power values in Fig. 8. As proved in [6], for any given number of stations, the protocol efficiency can reach up to 95% with suitable selection of code weight, code length and average peak laser power.

The effect of the light dispersion is shown in Fig. 9, the

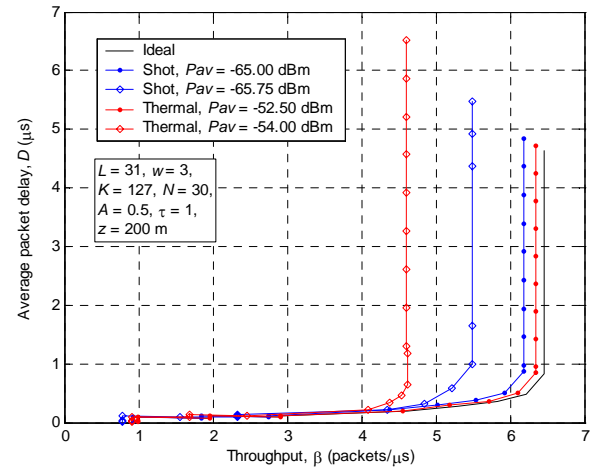


Fig. 7. Packet delay vs. throughput for different average peak laser power values.

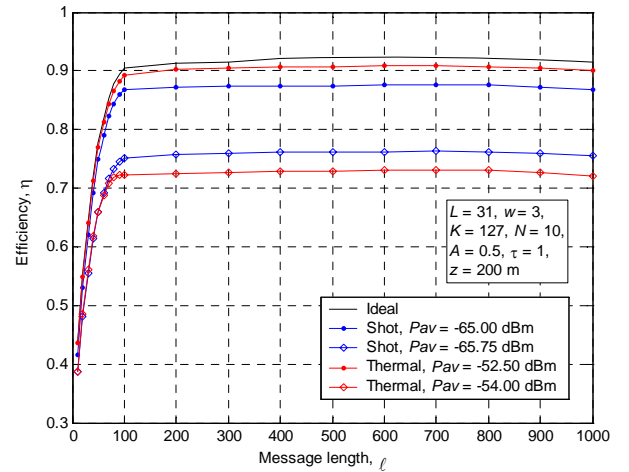


Fig. 8. Efficiency vs. message length for different average peak laser power values.

throughput has been plotted against the message length for various operating wavelengths $\lambda \in \{1550, 1300, 850\}$ nm, for two different interstation distances $z = \{200, 600\}$ m. As the message length is increased, the effect of MAI is also increased, and thus the throughput starts to fall as in [6], similar trends are noticed when the dispersion is considered but with lower values of throughput. If the operating wavelength is chosen in the 2nd window around the 1300 nm, the effect of the dispersion will be relatively small. If operated at the same wavelength, the throughput degradation will be significant for larger interstation distances; which verifies equations (21) and (24).

V- CONCLUSION

We have presented in this paper the performance degradation of the R^3T protocol. The effect of noise and light dispersion in fiber has been studied. The Poisson approximation and Gaussian approximation have been employed in our derivation of the performance of this protocol

taking into account the effect of shot noise and thermal noise, respectively. Finally the dispersion effect was considered.

The throughput, the average packet delay and the efficiency of the R^3T protocol have been derived, simulated and compared with the previous work in [6]. The following concluding remarks can be extracted from our results:

- 1- We can tolerate the effect of noise by reasonably increasing the average peak power at the transmitter to -63 dBm and -51 dBm for the case of shot noise and thermal noise respectively.
- 2- Shot noise saves 13 dB in power than thermal noise does for the same performance, i.e. the effect of the thermal noise on the performance degradation is much greater than that of the shot noise.
- 3- For small population networks, the effect of noise will be dominant, while for larger networks; the MAI is the main limiting factor.
- 4- The effect of both MAI and noise exhibits an acceptable average packet delay to the R^3T protocol performance.
- 5- An asymptotic efficiency of $\sim 95\%$ can be reached with suitable selection of code weight and code length.
- 6- It is clear that when operating in the 2nd window and for relatively small interstation distances (LAN), the dispersion effect will be negligible, so that the performance of the protocol will not be reduced very much.

REFERENCES

- [1] F. R. K. Chung, J.A Salehi, and V. K. Wei, "Optical orthogonal codes: Design, analysis and applications," *IEEE Trans. Inform. Theory*, vol. IT-35, pp. 595-604, May 1989.
- [2] J. A. Salehi and C. A Brackett, "Code division multiple-access techniques in optical fiber networks. Part II: systems performances analysis," *IEEE Trans. Commun.*, vol. COM-37, pp. 834-842, Aug. 1989.
- [3] C.-S. Hsu and V. O. K. Li, "Performance analysis of slotted fiber-optic code-division multiple-access (CDMA) packet networks," *IEEE Trans. Commun.*, vol. COM-45, pp. 819-828, July 1997.
- [4] C.-S. Hsu and V. O. K. Li, "Performance analysis of unslotted fiber-optic code-division multiple-access (CDMA) packet networks," *IEEE Trans. Commun.*, vol. COM-45, pp. 978-987, Aug. 1997.
- [5] H. M. H. Shalaby, "Optical CDMA random access protocols with and without pretransmission coordination," *IEEE/OSA J. Lightwave Technol.*, vol. LT-21, pp. 2455-2462, Nov. 2003.
- [6] H. M. H. Shalaby, "Performance analysis of an optical CDMA random access protocol," *IEEE/OSA J. Lightwave Technol.*, vol. LT-22, pp. 1233-1241, May 2004.
- [7] M. A. A. Mohamed, H. M. H. Shalaby, and E. A. El-Badawy, "Optical CDMA protocol with selective retransmission," in *Proc. Ninth IEEE Symp. On Computers and Communications (ISCC 2004)*, Alexandria, Egypt, June 29-July 1, 2004, pp. 621-626.

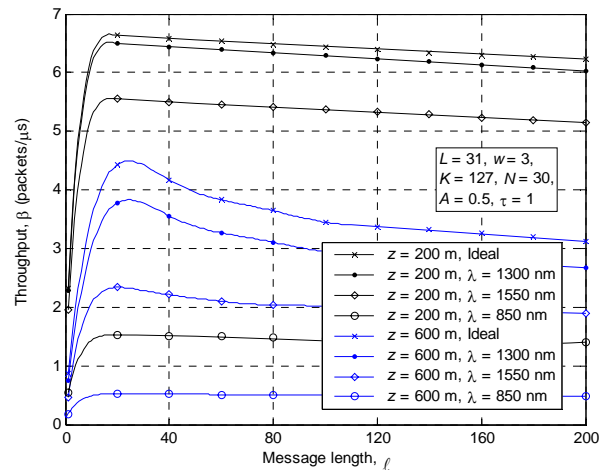


Fig. 9. Throughput vs. message length for different interstation distances and wavelengths.

- [8] H. M. H. Shalaby, "Chip-level detection in optical code-division multiple-access," *IEEE/OSA J. Light-wave Technol.*, vol. LT-16, pp. 1077-1087, June 1998.
- [9] H. M. H. Shalaby, "Complexities, error probabilities, and capacities of optical OOK-CDMA communication systems," *IEEE Trans. Commun.*, vol. COM-50, pp. 2009-2015, Dec. 2002.
- [10] V.F. B. Mezger and M. B. Pearce, "Dispersion limited optic-optic CDMA systems with overlapped signature sequences," in *Proc. IEEE Laser and Electro-Optics Soc. 9th Annu. Meeting*, 1996, pp. 408-409.
- [11] T. Pfeiffer, M. Witte, and B. Deppisch, "High-speed transmission of broadband thermal light pulses over dispersive fibers," *IEEE Photon. Technol. Lett.*, vol. 11, pp. 385-387, Mar. 1999.